Rhombohedral superhard structure of BC$_2$N

Quan Li,[1] Mei Wang,[1] Artem R. Oganov,[2,3] Tian Cui,[1] Yanming Ma,[1,a)] and Guangtian Zou[1]

[1]*National Laboratory of Superhard Materials, Jilin University, Changchun 130012, China*
[2]*Department of Materials, Laboratory of Crystallography, ETH Zurich, HCI G 515, Wolfgang-Pauli-Strasse 10, CH-8093 Zurich, Switzerland*
[3]*Department of Geology, Moscow State University, 119992 Moscow, Russia*

Ab initio evolutionary algorithm was employed to resolve the crystal structure of the observed superhard BC$_2$N. We uncovered two polymorphs with rhombohedral (2 f.u./cell) and orthorhombic (2 f.u./cell) symmetries, with which the experimental x-ray diffraction pattern is well reproduced. Analysis of the total energy results and the simulated energy-loss near-edge spectroscopy suggests that the rhombohedral structure is the best candidate for the superhard BC$_2$N. We further demonstrated that earlier proposed high density and low density forms are likely from this single rhombohedral phase. © *2009 American Institute of Physics*. [DOI: 10.1063/1.3086649]

I. INTRODUCTION

Due to the importance in fundamental science and technological applications, the search for superhard materials is an intriguing and long-standing problem, which has been greatly motivated following the synthesis of man-made diamonds and *c*-BN. It is known that superhard materials are usually made of light elements such as B, C, N, and O. Therefore, considerable efforts have been devoted to synthesizing various structured ternary B–C–N compounds by sintering various starting materials at high pressure and temperature. Among the ternary B–C–N compounds, diamondlike BC$_2$N (*c*-BC$_2$N) has gained extensive attention since it has been expected to be thermally and chemically more stable than diamond and harder than *c*-BN. Recently *c*-BC$_2$N has been synthesized[1–5] and the measured hardness reach 76 (Ref. 4) or 62 GPa,[5] indeed higher than *c*-BN. However, the crystal structure of *c*-BC$_2$N is still unknown since it remains a major challenge to determine the crystal structures of *c*-BC$_2$N from the experimental x-ray diffraction (XRD) patterns due to the similar and small atomic masses of B, C, and N atoms. On the theoretical side, many different crystal forms were proposed, e.g., zinc-blende struc-*m* (*m*=1–7),[6] chalcopyrite (cp-) BC$_2$N,[7] body-centered (bc6-) BC$_2$N,[8] tetragonal *z*-BC$_2$N,[9] wurtzite BC$_2$N,[10] and the short period (C$_2$)$_n$(BN)$_n$ (111) superlattices.[11] Among the proposed structures, *z*-BC$_2$N is constructed from the 16-atom supercell of diamond whose XRD spectrum agrees with the experiment data[4] very well, and the superlattices have the lowest energies. However, lack of any convincing XRD comparison with experimental data in the literature for this superlattice structural series[11] precludes full understanding of *c*-BC$_2$N and the intense debate still continues.[12,13] Therefore, the crystal structure of *c*-BC$_2$N is still far from being solved. Here, we have taken a route using our recently developed approach[14–16] to explore the crystal structures of *c*-BC$_2$N. First principles calculations were then performed to investi-gate the lattice parameters, bulk modulus, total energies, and hardness of the resultant structures. Electron energy-loss near-edge spectroscopy (ELNES) and XRD simulation are carried out to compare with the available experimental data.

II. METHODS

The structures of superhard BC$_2$N were predicted by the *ab initio* evolutionary methodology using USPEX code.[14–16] The most significant feature of this methodology is the capability of predicting the stable structure at given *P*/*T* conditions with only the knowledge of the *chemical composition*.[14–17] The calculations of the structure relaxations, band structures, and electronic density of states were carried out within the generalized gradient approximation as implemented in the Vienna *ab initio* simulation package (VASP).[18] The all-electron projector augment wave method[19] was adopted. We used the plane-wave kinetic energy cutoff energy of 1000 eV, which was shown to give excellent convergence of the total energies. The phonon frequencies for the energetically preferred BC$_2$N were calculated using direct supercell method as implemented in the PHON program.[20] This method uses the forces obtained by the Hellmann–Feynman theorem calculated from the optimized supercell. Convergence test gives the use of a supercell containing 64 atoms in the force constant calculation. The ELNES of the energetically preferred BC$_2$N is calculated by using the all-electron full potential linearized augmented plane-wave method, as implemented in the WIEN2K code.[21] To simulate the core-hole effect, the Slater transition state method[22] in which a half electron is removed from the core orbital to fill the lowest unoccupied orbital is employed. Moreover, in order to avoid the interactions between adjacent core holes, a $2 \times 2 \times 1$ supercell (96 atoms) is used. We convoluted theoretical spectra with a Gaussian contribution of 1.2 eV full width at half maximum Gaussian to take into account the instrumental line broadening. Theoretical XRD patterns of BC$_2$N are obtained by using the module of the Reflex in Materials Studio.[23]

a)Author to whom any correspondence should be addressed. Electronic mail: mym@jlu.edu.cn.

(a) *Pmm*2-1u
(b) *P*3*m*1-1u
(c) *R*3*m*-1u
(d) *Pmm*2-2u
(e) *P*3*m*1-2u
(f) *R*3*m*-2u
(g) *Pmm*2-4u
(h) *P*3*m*1-4u
(i) *R*3*m*-4u

● **B**   ● **C**   ● **N**
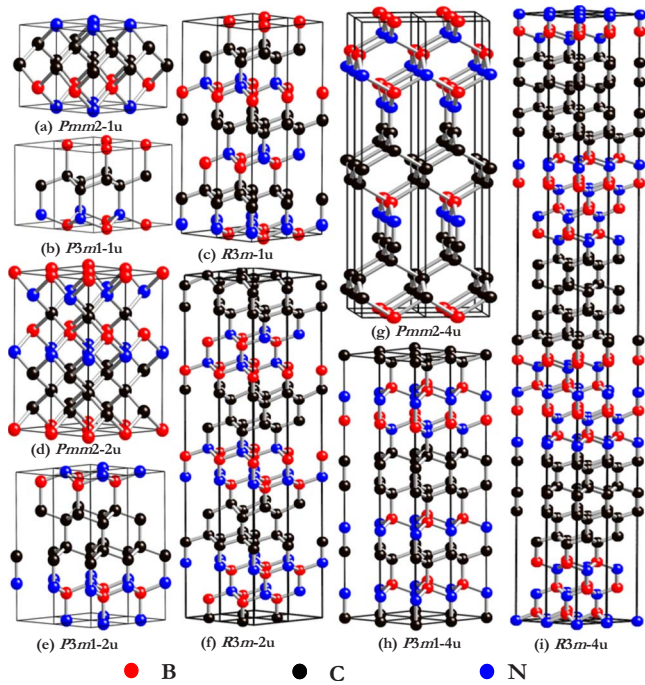
FIG. 1. (Color online) Crystal structures of c-BC_2N predicted by the current simulations.

III. RESULTS AND DISCUSSIONS

Since c-BC_2N is synthesized at high pressure (7.7–30 GPa),[1–5] we thus performed variable-cell structure prediction simulations at 30 and 100 GPa with systems containing 1, 2, and 4 f.u. in the simulation cell. We have revealed three structural series: orthorhombic $Pmm2$, hexagonal $P3m1$, and rhombohedral $R3m$. Figure 1 depicts the nine low-energy structures, namely, $Pmm2$-nu, $P3m1$-nu, and $R3m$-nu. Here n denotes the number of BC_2N units per primitive cell (n

$=1,2,4$). Except for $Pmm2$-$4u$, all the structures are tetrahedrally bonded with clear sp^3 hybridization. In our simulations, we have reproduced four structures proposed earlier: $Pmm2$-$1u$ is identical to struc-1,[6] $P3m1$-$1u$ is in accordance with the BC_2N-$w3$,[10] and $R3m1$-$1u$ and $R3m$-$2u$ have been proposed as $BC_2N_{1\times1}$ and $BC_2N_{2\times2}$,[11] respectively. The theoretical lattice parameters and the ratio (R) of stable bonds (C–C+B–N):less stable bonds (B–C+C–N) of the obtained BC_2N structures have been presented in Table I. Our calculations show that for the fixed number (n) of f.u. in the primitive cell, the most energetically favorable structures are $R3m$-nu, those with the maximized number of the stable B–N and C–C bonds. This fact is consistent with superlattice results.[11] Inspecting the crystal structure of $R3m$-$4u$ [Fig. 1(i)], a stacking of diamondlike and c-BN-like structure units is evidenced. With further increasing n, $R3m$ structure will possess even lower energy and at the limit of n infinite large, $R3m$ structure will eventually decompose into diamond +c-BN. Our current findings support the experimental observation[1] that c-BC_2N segregates into diamond and c-BN at high temperature and suggest that $R3m$ is a promising structure candidate for c-BC_2N. To solve the crystal structure of c-BC_2N, the experimental data of XRD or ELNES (Refs. 4 and 5) have to be relied on.

We have extensively simulated XRD patterns of the obtained structures and previously proposed best structures for c-BC_2N. The used x-ray wavelength (λ) is 0.3738 Å as employed in the experiments by Solozhenko *et al.*[4] It is found that among the proposed $R3m$-nu structures, only $R3m$-$2u$ structure reproduces the experimental XRD pattern[4] and other $R3m$-nu ($n \neq 2$) structures are thus eliminated. We have also ruled out the earlier proposed best structures, struct-1, BC_2N-$w3$, bc6-BC_2N, and cp-BC_2N, and the currently proposed $P3m1$-$2u$, $P3m1$-$4u$, and $Pmm2$-$4u$ by evidence of the

TABLE I. Calculated equilibrium structural parameters, total energies (E), the ratio (R) of stable bonds (C-C +B-N):less stable bonds (B-C+C-N), bulk modulus (B_0), and hardness (H) for the present and earlier proposed structures of BC_2N.

	Structure	a (Å)	b (Å)	c (Å)	V (Å³/f.u.)	E (eV/f.u.)	R	B_0 (GPa)	H (GPa)
BC_2N	$Pmm2$-$1u$	2.565	2.538	3.645	23.727	−33.901	1:1	371	71.0
	$P3m1$-$1u$	2.531	2.531	4.248	23.567	−34.842	3:1	389	61.2
	$R3m$-$1u$	2.540	2.540	12.541	23.509	−34.897	3:1	391	61.5
	$Pmm2$-$2u$	2.562	2.557	7.270	23.810	−33.690	1:1	369	70.8
	$P3m1$-$2u$	2.540	2.540	8.397	23.448	−35.140	7:1	396	62.0
	$R3m$-$2u$	2.545	2.545	25.068	23.443	−35.155	7:1	395	62.1
	$Pmm2$-$4u$	2.626	2.537	15.133	25.203	−34.517	⋯	331	⋯
	$P3m1$-$4u$	2.532	2.532	16.942	23.518	−34.962	13:3	399	61.5
	$R3m$-$4u$	2.541	2.541	50.314	23.407	−35.246	15:1	397	62.2
	z-BC_2N	3.604	3.604	7.247	23.536	−34.689	3:1	385	65.0
	bc6-BC_2N(A)	4.419	4.424	4.453	29.027	−33.251	2:1	292	55.1
	cp-BC_2N	3.653	3.653	7.228	24.114	−32.299	0	349	67.5
Diamond	Theor.	3.569			11.366	−18.195		423	92.1
	Expt.	3.567[a]			11.346			443[a]	96±5 [b]
c-BN	Theor.	3.624			11.899	−17.426		370	58.6
	Expt.	3.617[c]			11.830			368[c]	63±5 [b]

[a]Reference 26.
[b]Reference 27.
[c]Reference 2.
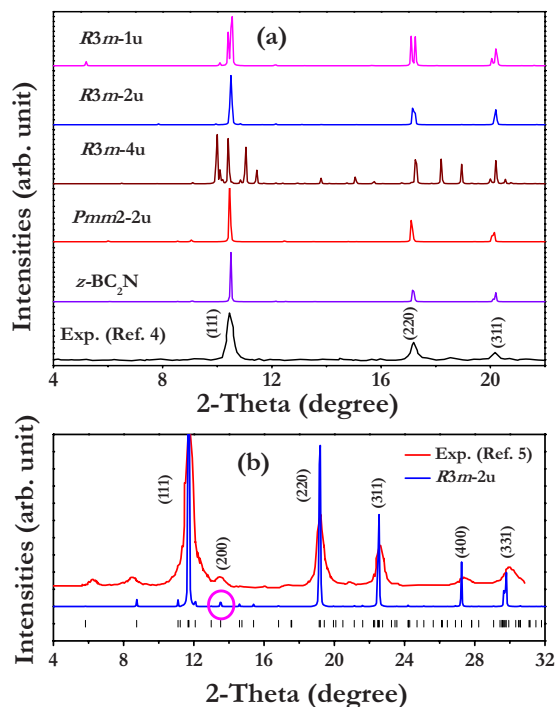
FIG. 2. (Color online) Simulated XRD patterns of the currently predicted and earlier proposed structures with λ=0.3738 (a) and 0.4246 Å (b). The experimental XRD spectrum from Refs. 4 and 5 is also shown for comparison.

FIG. 3. (Color online) The theoretical B, C, and N K-edge spectra for $R3m$-2u BC_2N to compare with the experimental data (Ref. 5). The calculated ELNES has been shifted and aligned with the experimental data.

mismatching XRD pattern with experimental data. Note that our predicted $Pmm2$-2u and earlier z-BC_2N could also reproduce the experimental pattern [Fig. 2(a)]. However, the enthalpies for $R3m$-2u are 1.465 and 0.466 eV lower than those of $Pmm2$-2u and z-BC_2N, respectively. These large energy differences indicate a much more preferable formation of $R3m$-2u structure. For the entropic effects to overcome the large energy difference of 0.466 eV, temperatures of the order of 5×10^3 K are needed. However, none of experimental synthesis is performed at such high temperatures. Zhao *et al.*[5] reported an additional (200) peak in the XRD pattern of their synthetic sample. Further consideration of their resulting slightly smaller (0.047 Å) lattice parameter and larger bulk modulus, it is argued that their synthetic material is a high density (HD) form, in contrast to that a low density (LD) phase synthesized by Solozhenko *et al.*[4] In order to clarify this discrepancy, we have also simulated XRD patterns of $R3m$-2u structure with λ=0.4246 Å used by Zhao *et al.*[5] [Fig. 2(b)]. Remarkably, the simulated XRD peak positions and relative intensities match the experimental data[5] very well. The (200) peak is clearly revealed although it is rather weak. We then carefully re-examined the simulated XRD pattern [Fig. 2(a)] with λ=0.3738 Å. The (200) peak is also evidenced and the extremely weak intensity of (200) peak might explain the failure of observation in Ref. 4. With the current structural model of $R3m$-2u, both measured XRD patterns in Refs. 4 and 5 are reasonably understood. It is very important to point out that most characteristic of structure is the XRD pattern, while neither the lattice parameter nor the bulk modulus. Therefore, we suggest that the previously proposed HD and LD forms might be originated from the single phase of $R3m$-2u structure. In fact, the observed discrepan-

cies of lattice parameters, hardness, and bulk modulus are understandable by the big difficulty in synthesizing the crystalline B–C–N phase with high purity and large block, which results in some uncertainty of experimental measurements. Further fine experimental measurements are thus demanded to clarify these discrepancies.
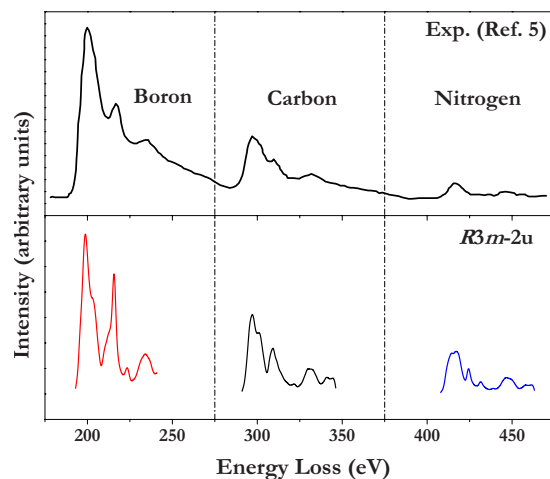
The available experimental ELNES data[5] allow us to further confirm our conclusion. The simulated B, C, and N K-edge spectra of $R3m$-2u BC_2N together with the experimental spectra are shown in Fig. 3. One observes that with the $R3m$-2u structure, the experimental peak positions, shapes, and intensities are all well reproduced, lending another strong support for the validity of the current structure model. Our calculations also confirmed that there is no π^* bonding feature in c-BC_2N and the first strong peaks correspond to the transitions of 1s electrons to the empty σ^* antibonding orbitals (sp^3 bonding).

The total energies as a function of volume are fitted to the Murnaghan equation of state to obtain the theoretical bulk modulus (B_0), as listed in Table I. The calculated bulk modulus of $R3m$-2u BC_2N is 395 GPa, which is in good accordance with the experimental value of 401 GPa by Komatsu *et al.*[3] but much higher than that of 282 GPa by Solozhenko *et al.*[4] The hardness calculations were performed with the Šimůnek–Vackář model.[24] The theoretical hardness of $R3m$-2u BC_2N is 62.1 GPa, in excellent agreement with the experimental value of 62 (Ref. 5) or 76 GPa.[4] It is significant to note that the hardness of BC_2N within $R3m$-2u structure exceeds than that of c-BN (58.6 GPa) in this calculation, which is consistent with the experimental result.[4,5]

To have further insights into $R3m$-2u BC_2N, the calculated band structures, total and partial densities of states (DOSs), at zero pressure have been presented in Fig. 4. The band structures indicate that the $R3m$-2u BC_2N is a wide gap semiconductor with an indirect band gap of 3.8 eV as shown in Fig. 4(a). Due to the well-known band gap underestimation in density functional theory (DFT), the true energy gap of $R3m$-2u structure should be, in fact, larger. This is consistent with the experiment observations.[4,5] From the DOS plots [Fig. 4(b)], it is found that the lower valence bands are
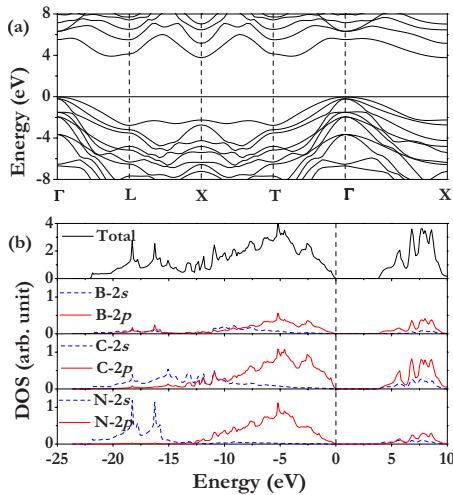
FIG. 4. (Color online) The calculated band structures (a) and electron partial density of states (b) for $R3m$-$2u$ BC$_2$N.

mainly from $2s$ electrons of C and N atoms. For the higher valence bands, the main contributions come from the $2p$ electrons of B, C, and N atoms, in contrast to the obviously small contributions from $2s$ electrons. This is consistent with the charge transfer from $2s$ to $2p$ due to the sp^3 hybridization. The conduction bands are mainly originated from $2p$ and $2s$ orbitals and are of σ^* character.

It is known that the lattice dynamical stability requires that the energies of phonons must be positive for all wave vectors in the Brillouin zone (BZ).[25] To check the dynamical stability of $R3m$-$2u$ structure, we calculated the phonon dispersion curves and projected phonon DOS (PPDOS) at zero pressure as shown in Fig. 5. Since there are eight atoms in the primitive cell, we have 3 acoustic and 21 optic phonon branches. From the PPDOS [Fig. 5(b)], it is found that there is a strong coupling among B, C, and N atoms due to their similar atomic masses. No imaginary phonon frequencies are observed in the whole BZ, indicating that the $R3m$-$2u$ structure is dynamically stable.

IV. CONCLUSION

To conclude, we have demonstrated that the $R3m$-$2u$ structure is likely the structure of superhard BC$_2$N. Our results support the earlier superlattice structural models. Importantly, we have pointed out that the previously suggested
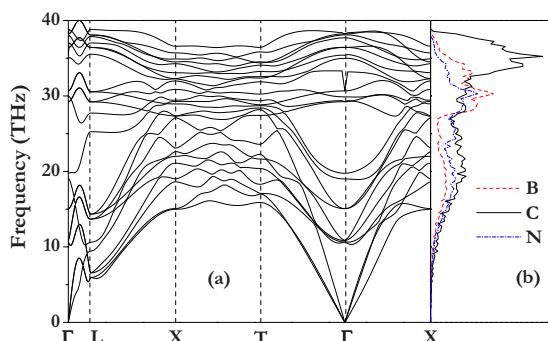
FIG. 5. (Color online) The calculated phonon dispersion curves (a) and projected phonon density of states (b) for $R3m$-$2u$ BC$_2$N.

HD and LD forms could be originated from the single $R3m$-$2u$ phase. The hardness simulation indicates that $R3m$-$2u$ BC$_2$N has surpassed c-BN as the second highest hardness material. The calculated electronic structures show that $R3m$-$2u$ BC$_2$N is a wide gap semiconductor with an indirect DFT band gap of 3.8 eV. The structure stability of $R3m$-$2u$ BC$_2$N has been confirmed by the calculation of phonon frequencies. It is thus greatly motivated to explore the potential technological and industrial applications in c-BC$_2$N.

[1] S. Nakano, M. Akaishi, T. Sasaki, and S. Yamaoka, Chem. Mater. **6**, 2246 (1994).
[2] E. Knittle, R. B. Kaner, R. Jeanloz, and M. L. Cohen, Phys. Rev. B **51**, 12149 (1995).
[3] T. Komatsu, M. Nomura, Y. Kakudate, and S. Fujiwara, J. Mater. Chem. **6**, 1799 (1996).
[4] V. L. Solozhenko, G. Andrault, G. Fiquet, M. Mezouar, and D. C. Rubie, Appl. Phys. Lett. **78**, 1385 (2001).
[5] Y. Zhao, D. W. He, L. L. Daemen, T. D. Shen, R. B. Schwarz, Y. Zhu, D. L. Bish, J. Huang, J. Zhang, G. Shen, J. Qian, and T. W. Zerda, J. Mater. Res. **17**, 3139 (2002).
[6] H. Sun, S.-H. Jhi, D. Roundy, M. L. Cohen, and S. G. Louie, Phys. Rev. B **64**, 094108 (2001).
[7] X. F. Z. J. Sun, G. R. Qian, J. Chen, Y. X. Fan, H. T. Wang, X. J. Guo, J. L. He, Z. Y. Liu, and Y. J. Tian, Appl. Phys. Lett. **89**, 151911 (2006).
[8] X. Luo, X. Guo, B. Xu, Q. Wu, Q. Hu, Z. Liu, J. He, D. Yu, Y. Tian, and H. Wang, Phys. Rev. B **76**, 094103 (2007).
[9] X. Zhou, J. Sun, Y. Fan, J. Chen, H. Wang, X. Guo, J. He, and Y. Tian, Phys. Rev. B **76**, 100101(R) (2007).
[10] X. Luo, X. Guo, Z. Liu, J. He, D. Yu, B. Xu, Y. Tian, and H. Wang, Phys. Rev. B **76**, 092107 (2007).
[11] S. Chen, X. G. Gong, and S.-H. Wei, Phys. Rev. Lett. **98**, 015502 (2007).
[12] C. Chen and H. Sun, Phys. Rev. Lett. **99**, 159601 (2007).
[13] S. Chen, X. G. Gong, and S.-H. Wei, Phys. Rev. Lett. **99**, 159602 (2007).
[14] A. R. Oganov and C. W. Glass, J. Chem. Phys. **124**, 244704 (2006).
[15] C. W. Glass, A. R. Oganov, and N. Hansen, Comput. Phys. Commun. **175**, 713 (2006).
[16] A. R. Oganov, C. W. Glass, and S. Ono, Earth Planet. Sci. Lett. **241**, 95 (2006).
[17] Y. M. Ma, A. R. Oganov, and C. W. Glass, Phys. Rev. B **76**, 064101 (2007).
[18] G. Kresse and D. Joubert, Phys. Rev. B **59**, 1758 (1999).
[19] P. E. Blöchl, Phys. Rev. B **50**, 17953 (1994).
[20] D. Alfè, http://chianti.geol.ucl.ac.uk/~dario.
[21] P. Blaha, K. Schwarz, G. Madsen, D. Kvasnicka, and J. Luitz, *WIEN2K: An Augmented-Plane-Wave+Local Orbitals Program for Calculating Crystal Properties* (Karlheinz Schwarz, Wien, Austria, 2001).
[22] J. C. Slater, *Quantum Theory of Molecules and Solids* (McGraw-Hill, New York, 1974).
[23] M. D. Segall, P. L. Lindan, M. J. Probert, C. J. Pickard, P. J. Hasnip, S. J. Clark, and M. C. Payne, J. Phys.: Condens. Matter **14**, 2717 (2002).
[24] A. Šimůnek and J. Vackář, Phys. Rev. Lett. **96**, 085501 (2006).
[25] G. A. Samara and P. S. Peercy, in *Solid State Physics*, edited by H. Ehrenreich, F. Seitz, and D. Turnbull (Academic, New York, 1981), Vol. 36.
[26] M. T. Yin, Phys. Rev. B **30**, 1773 (1984).
[27] R. A. Andrievski, Int. J. Refract. Met. Hard Mater. **19**, 447 (2001).